Calculations of the electronic structure and superconducting properties of the Ba(K)Pb(Bi)O_3 system

D. A. Papaconstantopoulos
Naval Research Laboratory, Washington, D.C. 20375-5000

A. Pasturel, J. P. Julien, and F. Cyrot-Lackmann
Laboratoire d'Etudes des Propriétés Electroniques des Solides, Centre National de la Recherche Scientifiques, 25 Avenue des Martyrs, BP166-38042, Grenoble, France

(Received 15 May 1989)

We have performed band-structure calculations of the cubic perovskites $BaPbO_3$, $BaBiO_3$, and $KBiO_3$ by the augmented-plane-wave (APW) method. Using the APW results, we have constructed the first realistic tight-binding (TB) Hamiltonians for these materials including the s (Ba or K) orbitals, the s and p (Pb or Bi) orbitals, and the p (O) orbitals. These TB Hamiltonians were used to apply the coherent-potential approximation to study disorder effects. We found that, while the position of the Fermi level moves qualitatively according to the rigid-band approximation, the oxygen-dominated bandwidth widens as a result of alloying either on the Ba or the Bi sites. Our evaluation of the electron-phonon coupling indicates that this is a possible mechanism to explain superconductivity in these systems.

I. INTRODUCTION

Superconductivity near 30 K was discovered recently[1,2] in a copper-free phase, $Ba_{1-x}K_xBiO_3$. This discovery is quite remarkable as it is the first copper-free oxide superconductor that has a transition temperature above that for the best intermetallic superconductors and its structure is cubic. But this material also has common properties with the cuprate high-T_c superconductors and with $BaPb_{1-x}Bi_xO_3$, which has a T_c of 12 K, such as the occurrence of superconductivity close to a metal-insulator transition.[3] This transition is thought to be accompanied in the cuprates by a strong-correlation Coulomb repulsion (the parent pure compounds being insulating and antiferromagnetic), and in the Bi-free copper systems by a charge-density wave (CDW). $BaBiO_3$ is known to be an insulator with a CDW gap of 2 eV.[4,5] The apparent absence of magnetic order in (Ba,K)BiO_3 (Ref. 6) and the large isotope effect[7] leads some authors to the idea that the pairing mechanism might be conventional (phonon mediated). But there are still many puzzling questions regarding these materials, such as the importance of the cubic structure, the relation with the CDW, and the large resistivity behaving like a doped semiconductor above T_c.[8] Some of these questions may be resolved from a good understanding of the electronic structure of these materials.

Band-structure calculations for $BaPbO_3$ were published in the early 1980's by Mattheiss and Hamann.[9] These calculations were performed by the linearized augmented-plane-wave (LAPW) method and utilized the virtual-crystal approximation to treat the disordered compounds $BaPb_{1-x}Bi_xO_3$. These authors used the LAPW approach to calculate the electronic structure for the high-temperature cubic phase as well as the room-temperature tetragonal and monoclinic phases. The crystallographic studies of Cox and Sleight[10] have shown that this system is orthorhombic for small x, and it becomes tetragonal in the range $0.05 < x < 0.35$ (where it is found to be superconducting). At $x = 0.35$ it returns to an orthorhombic phase which is accompanied by a metal-semiconductor transition. For $x > 0.9$ it remains a semiconductor but it goes to a monoclinic phase.

Mattheiss and Hamann[9] found very small changes between the band structure of the cubic phase and that of the tetragonal phase in $BaPbO_3$. However, in $BaBiO_3$ their calculation in the monoclinic phase showed energy-band splittings that produced a small gap at the Fermi level (E_F), consistent with observed semiconducting properties at this end of the compositional spectrum. In 1987 Takegahara and Kasuya[11] reported augmented-plane-wave (APW) calculations for $BaPbO_3$, $BaBiO_3$, and $BaPb_{0.5}Bi_{0.5}O_3$ in a supercell structure. Their results are fairly similar to those of Mattheiss and Hamann but they argue that they have better agreement with photoemission measurements. They also claim that the origin of the semiconducting properties of this system is due to a spin-density-wave formation on Bi sites.

Very recently the discovery[1,2] of high-temperature superconductivity in cubic $Ba_{1-y}K_yBiO_3$ renewed the interest in this class of materials. Mattheiss and Hamann[12] again, performed LAPW calculations for ordered $Ba_{0.5}K_{0.5}BiO_3$ alloys and showed that the antibonding Bi($6s$)-O($2p$) conduction band near E_F is nearly the same as in $BaBiO_3$. They point out that this supports the prediction that doping of the Ba site extends the metallic range of this alloy closer to half-filling than the doping of the Bi site does, and therefore maximizes the electron-phonon interaction.

In this work we performed APW band-structure calcu-

lations for $BaPbO_3$, $BaBiO_3$, and $KBiO_3$ and fit them to a tight-binding (TB) Hamiltonian of Slater-Koster.[13] These TB Hamiltonians were then used as the basis of calculations of disordered $BaPb_{1-x}Bi_xO_3$ and $Ba_{1-y}K_yBiO_3$ alloys with the coherent potential approximation (CPA) method.[14]

II. COMPUTATIONAL DETAILS

We performed APW calculations of the band structure of the cubic perovskites $BaPbO_3$, $BaBiO_3$, and $KBiO_3$ in the muffin-tin (MT) approximation. The MT approximation (spherical symmetry of the charge density and potential inside the MT spheres and constant potential in the interstitial region) is very reliable for cubic materials. Therefore, we prefer to use our faster symmetrized APW codes for these calculations than the LAPW approach which usually removes the MT approximation and is more accurate for noncubic systems. Our choices of lattice parameters and MT radii are given in Table I.

Our APW calculations are scalar relativistic, i.e., include the mass velocity and Darwin terms in the Hamiltonian but neglect the spin-orbit interaction. In Table II we show the levels that were treated as bands by the APW method. The inner levels were not frozen but recalculated in each iteration by an atomic structure code that included the spin-orbit interaction. The exchange and correlation term of the potential was treated in the local density approximation using the procedure of Hedin and Lundqvist.[15] The iterations to self-consistency were done on a uniform mesh of 10 k points in the $\frac{1}{48}$th of the Brillouin zone (BZ). It required 20 iterations with simple mixing of the charge densities to achieve convergence to within 3 mRy. Once self-consistency was achieved the final potential was used to generate eigenvalues for 35 k points in the irreducible BZ.

The APW eigenvalues at 35 k points were used to perform a Slater-Koster (SK) fit according to the following procedure. We construct a 14×14 tight-binding Hamiltonian which includes the s Ba(K), s,p Pb(Bi), and p O orbitals. This Hamiltonian is orthogonal and contains 17 two-center parameters that were determined by a least-squares fit to the APW eigenvalues. The rms fitting error was approximately 10 mRy for the first ten bands and for all the three compounds. In Table III we present the values of the SK parameters.

The densities of states (DOS's) were calculated using two different procedures. The first one, which we will refer to as APW-DOS, interpolates the APW results (35 k-point mesh) onto a mesh of 165 k points in the irreducible BZ. This step is performed by the method of Boyer[16] which consists of a Fourier series interpolation with the symmetry of the different bands built in. The second step uses the interpolated eigenvalues and the l components of the MT charges as weights, to apply the tetrahedron method[17] for the determination of the DOS.

In the second procedure, referred to as SK-DOS, we use our SK parameters to diagonalize the 14×14 SK Hamiltonian again for 165 k points. The eigenvectors of the SK matrix give the necessary decomposition of l character. The second step is the same as in the first procedure, that is we use the tetrahedron method with the SK results as input.

The third part in our calculations is the application of the CPA (Ref. 14) to obtain the electronic states of the disordered phases of the above compounds. The basic assumption of the CPA is that the average scattering of electrons off the atomic sites is equal to zero. This can be mathematically stated by the following matrix equation:

$$x\frac{\varepsilon_A-\Sigma}{1-(\varepsilon_A-\Sigma)G}+(1-x)\frac{\varepsilon_B-\Sigma}{1-(\varepsilon_B-\Sigma)G}=0\ , \qquad (1)$$

where x is the concentration, ε_A and ε_B are the on-site SK parameters for the components A and B, Σ is the CPA self-energy, and G is the effective Green's function which is given by an integral over the BZ as follows:

$$G=\int_{\mathrm{BZ}}\frac{dk}{z-\overline{H}(k)}\ , \qquad (2)$$

where z is the complex energy and $\overline{H}(k)$ is an effective Hamiltonian found from the unperturbed Hamiltonian by replacing $\varepsilon_{A,B}$ by Σ. To approximate the effects of off-diagonal disorder we have used a concentration weighted average of the hopping parameters of Table III according to the expression,

$$\ln W=x\ln W_A+(1-x)\ln W_B\ .$$

An iterative procedure between Eqs. (1) and (2) gives the value of Σ as a function of energy and the 14×14 matrix G.

In the present application for $BaPb_{1-x}Bi_xO_3$ the CPA is applied on the s and p orbitals of Pb and Bi and therefore we work with two equations of the form (1) and need to determine two self-energies $\Sigma_s(E)$ and $\Sigma_p(E)$. In the $Ba_{1-y}K_yBiO_3$ alloy we have only the s-like orbital of Ba and K and hence one self-energy $\Sigma_s(E)$. Having determined the matrix G, it is a straightforward matter to calculate the densities of states for each angular momentum component by taking the usual trace of the imaginary part of G.

TABLE I. Lattice constants a and MT radii R in atomic units.

	$BaPbO_3$	$BaBiO_3$	$KBiO_3$
a	8.0635	8.2203	8.1069
R_{Ba}	3.6859	3.7576	3.7057
R_{Pb}	2.0159	2.0551	2.0267
R_O	2.0159	2.0551	2.0267

TABLE II. Levels calculated as bands by the APW method.

Ba	5s	5p	6s
Pb(Bi)	5d	6s	6p
O	2s	2p	

TABLE III. Slater-Koster parameters expressed in Ry.

	$BaPbO_3$	$BaBiO_3$	$KBiO_3$	MH[a]
		On-site energies		
s (Ba,K)	0.6832	0.7077	0.5976	
s (Pb,Bi)	0.4960	0.1859	0.2237	−0.301
p (Pb,Bi)	1.0857	1.9395	2.2566	0.257
p (O)	0.3498	0.3108	0.2861	−0.140
		First-neighbor hopping integrals		
$ss\sigma$ Ba(K)-Ba(K)	−0.0325	−0.0641	−0.0226	
$ss\sigma$ Pb(Bi)-Pb(Bi)	−0.0046	−0.0140	−0.0102	
$sp\sigma$ Pb(Bi)-Pb(Bi)	0.0020	−0.0503	0.0252	
$pp\sigma$ Pb(Bi)-Pb(Bi)	−0.0973	−0.1097	0.0345	
$pp\pi$ Pb(Bi)-Pb(Bi)	0.0322	0.0342	0.1329	
$pp\sigma$ O-O	0.0510	0.0408	0.0368	
$pp\pi$ O-O	0.0159	0.0039	−0.0067	
$ss\sigma$ Ba(K)-Pb(Bi)	−0.0088	0.0108	0.0252	
$sp\sigma$ Ba(K)-Pb(Bi)	−0.0242	−0.0124	−0.0281	
$sp\sigma$ Ba(K)-O	0.0500	0.0434	0.0168	
$sp\sigma$ Pb(Bi)-O	−0.1463	−0.1543	−0.1517	−0.162
$pp\sigma$ Pb(Bi)-O	0.1361	0.2047	0.2031	0.199
$pp\pi$ Pb(Bi)-O	0.0828	0.0314	−0.0624	−0.066

[a]Mattheiss-Hamann model.

III. DISCUSSION OF RESULTS

A. APW results

Before we proceed with a comparison of our valence bands with those presented by Mattheiss and Hamann[9] and by Takegahara and Kasuya[11] we wish to point out that these three sets of calculations were performed with different procedures which introduce several quantitative differences in the results. The calculational differences are the following.

(a) In Ref. 1 the LAPW approach that is used eliminates the shape approximation to the potential. This work and that of Ref. 3 employ the MT approximation.

(b) The size of the MT radii is different in the three sets of calculations.

(c) Both Refs. 9 and 11 make the frozen core approximation, while we recalculate the core levels in each iteration.

(d) The exchange and correlation potential is calculated by the Wigner interpolation formula in Ref. 9, by the Gunnarson-Lundqvist prescription in Ref. 11, and by the Hedin-Lundqvist approach in our work.

(e) In Ref. 9 the charge density for each iteration was determined using four special k points, while in Ref. 11 and our work, a uniform mesh of 10 k points was used.

(f) The number of first-principles k points used as input to calculate the density of states, and the method of calculating the DOS, were different in all three calculations.

The above differences in the computational procedures should account for the generally small discrepancies between the calculations discussed later.

In Figs. 1–3 we present the energy bands as determined by our APW calculations. In Fig. 1, for $BaPbO_3$, we show the so-called semicore states in addition to the valence bands. The lowest-lying states in this figure, centered at approximately −0.8 Ry, originate from the 2s O level. The states in the energy range −0.7–−0.5 Ry correspond to the 5d levels of Pb. The next narrow bands at about −0.2 Ry are the 5p levels of Ba. The 5s levels of Ba that we also treated as bands in our calculations are not shown in Fig. 1; they are deeper in energy at about −1.3 Ry. Comparing the valence bands of Fig. 1 with those given in Refs. 9 and 11 we note that near E_F all calculations are in good agreement and therefore they would predict almost identical Fermi surfaces. Away from E_F a major reordering of levels occurs which can be identified at Γ_1. Reference 11 and this work place Γ_1 between Γ_{25} and Γ_{15}, while in Ref. 9 Γ_1 lies below Γ_{25}. Partial-wave analysis of the bands reveals that in all calculations the states below and near E_F are dominated by 2p O contributions with smaller s Ba and s,p Pb character.

In Fig. 2 we show the energy bands of $BaBiO_3$. In this figure we do not show all the semicore levels but it is worth mentioning that the 5d Bi states are deeper in energy than the 5d Pb levels in $BaPbO_3$. In fact, these states lie below the 2s O levels and close to the 5s Ba. There are two major differences in the band structure of $BaBiO_3$ as compared with that of $BaPbO_3$. First, close to the point R, the 5p Ba semicore states overlap with the 6s Bi levels, and second the Γ_1 state falls below the Γ_{15} level. Mattheiss and Hamann[9] argue that the position of the Γ_1 state with respect to E_F determines whether these materials are semimetallic or semiconducting. The energy bands resulting from the present calculations and those of Refs. 9 and 11 are in good agreement for $BaBiO_3$. It should be mentioned however, that Mattheiss and

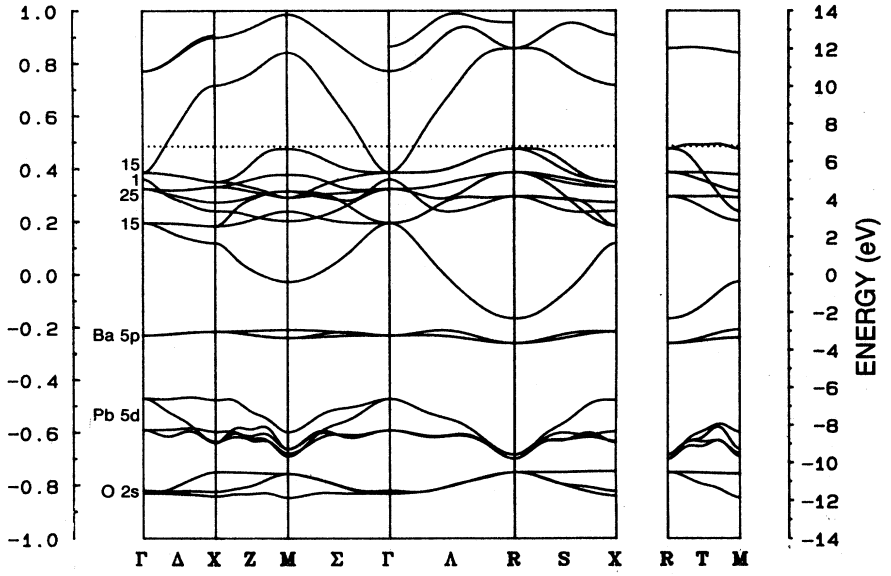

FIG. 1. Energy bands of $BaPbO_3$.

Hamann in Ref. 12 report a calculation for $BaBiO_3$ with a 1.4% smaller lattice constant, in which the levels Γ_1 and Γ_{15} are switched.

In Fig. 3 we show the energy bands of $KBiO_3$. We note first that near E_F the bands are very similar to those of $BaPbO_3$, which has the same number of electrons as $KBiO_3$. The bands from -0.3 to 0.3 Ry are very similar to those of $BaBiO_3$. On the other hand, the bands centered at -0.8 Ry represent the $2s$ O states, while the $5d$ Bi states are not shown in this figure since they are much deeper in energy unlike the situation in $BaPbO_3$.

In Fig. 4 we show the APW-DOS for $BaBiO_3$ and $KBiO_3$. The peaks centered at about -0.8 and -0.3 Ry describe the $2s$ O and the $5p$ Ba($3p$ K) semicore states. At higher energies we find the $2p$ O states that cover the energy range from 0 Ry to E_F. At E_F, for $BaBiO_3$ we have s Bi presence, which is approximately 25% of the p O component. However, in both $BaPbO_3$ and $KBiO_3$ the DOS at E_F has 90–95 % p O character.

B. The Slater-Koster results

As discussed in Sec. II the APW results were used to obtain a SK Hamiltonian for the three compounds. We

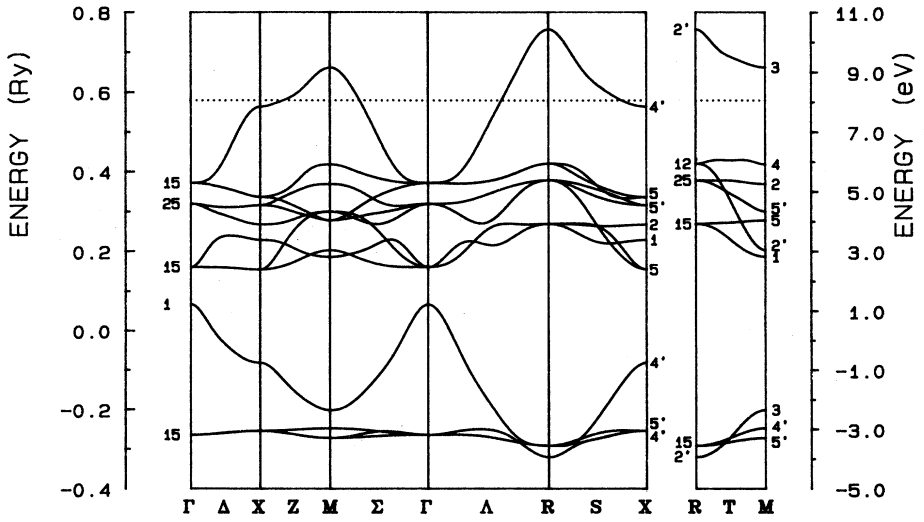

FIG. 2. Energy bands of $BaBiO_3$.

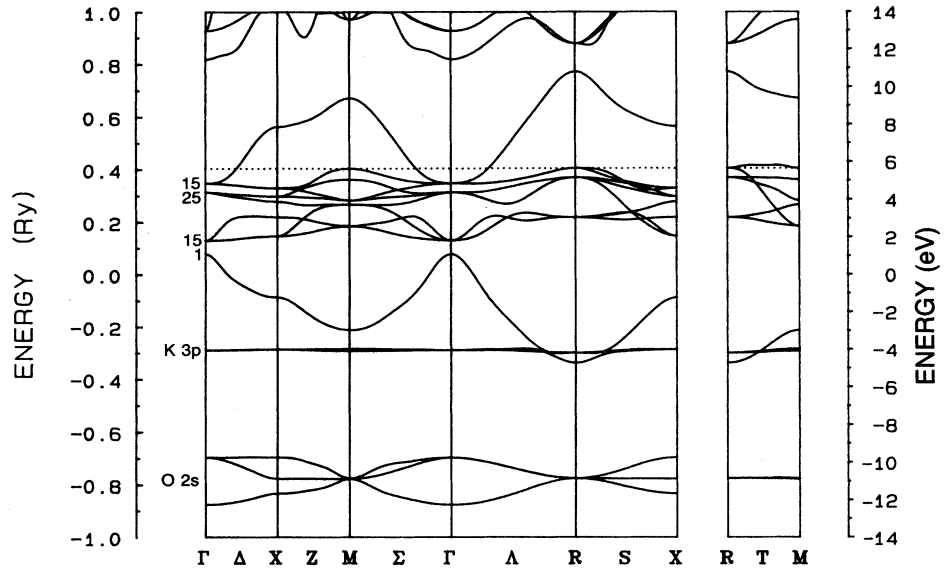

FIG. 3. Energy bands of $KBiO_3$.

first wish to comment on the TB Hamiltonian constructed by Mattheiss and Hamann (MH).[9] They have proposed a simple Hamiltonian based on six parameters that includes the s and p on-site energies of Pb (or Bi) the p O on-site energy and the $sp\sigma$, $pp\sigma$, and $pp\pi$ hopping integrals between Pb and O. Their assumption that the strongest interactions are the $sp\sigma$, $pp\sigma$, and $pp\pi$ between Pb and O, is supported by our work, as can be seen from Table III. However, the other interactions that we have included are far from being negligible. We note that the apparent disagreement in the size of the on-site energies is not very significant because it is mainly due to different APW energy scales. The MH approach gives a DOS for $BaPbO_3$ (and for $BaBiO_3$ by a rigid-band shift of E_F), which is shown in Fig. 5. From this figure we have omitted the nonbonding O $2p$ bands that are degenerate and appear as a δ function at an energy equal to -0.14 Ry. Our SK-DOS for $BaPbO_3$ are shown in Fig. 6. A com-

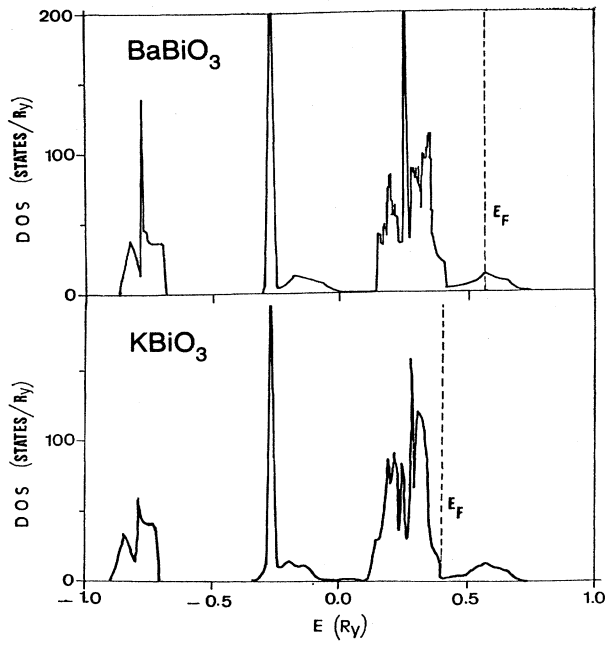

FIG. 4. APW total density of state for $BaBiO_3$ and $KBiO_3$.

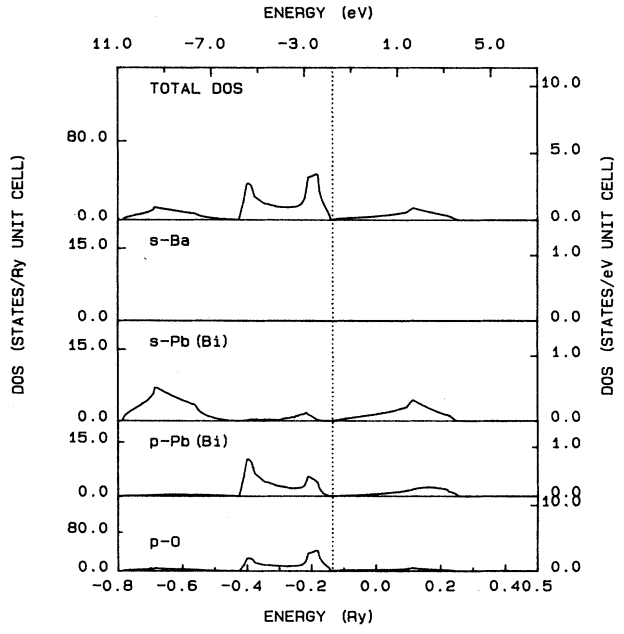

FIG. 5. Total and partial densities of state using the tight-binding parameters of Ref. 9.

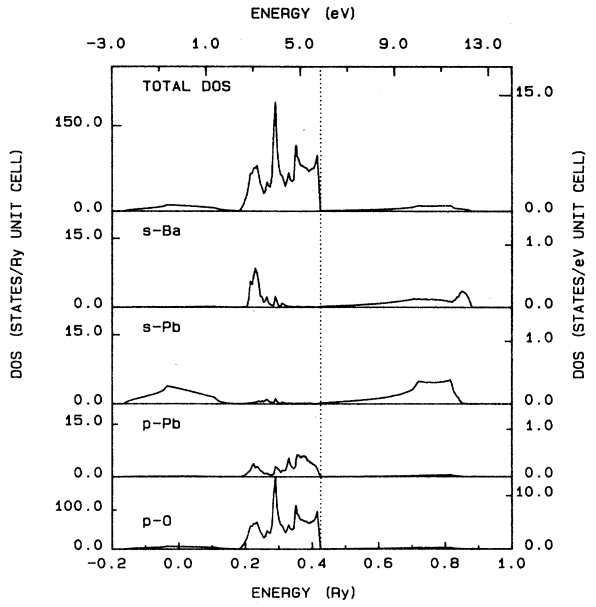

FIG. 6. Slater-Koster densities of state for $BaPbO_3$.

parison of Figs. 5 and 6 shows that the simplified parametrization of Mattheiss and Hamann can only give a qualitative picture of the DOS in this compound. The detailed structure both in the total and the O DOS is absent in the MH model. The *s* Pb DOS is reproduced rather well but the *s* Ba is not included. In Fig. 7 we show the SK-DOS for $BaBiO_3$. A comparison of Figs. 6 and 7 reveals, to some first-order approximation, a rigid-band behavior. The Fermi level moves to a higher energy to accommodate the extra electron of Bi. The structure of the total DOS is similar but with substantial differences in the relative heights of the peaks. The O- *p* DOS in both compounds is the main contributor to the total DOS, and has almost identical structure to that of the total DOS. The other *l* components of the DOS are very small. There are some small differences between the two compounds. For example, the *s* Ba DOS shows a contribution above E_F only for $BaPbO_3$. More importantly, at E_F there is a significant contribution from *s* Bi states in $BaBiO_3$, which is absent in $BaPbO_3$.

An examination of Fig. 8, which shows the DOS of $KBiO_3$, and a comparison with the DOS of its isoelectronic counterpart $BaPbO_3$ reveals many similarities. A comparison of the DOS of $KBiO_3$ with that of $BaBiO_3$ demonstrates rigid-band characteristics. A comparison of the SK-DOS shown in Figs. 6–8 with the APW-DOS of Fig. 4, shows good agreement in the main structure of the total DOS and consistency in features such as the strong participation of the *p* O states and the *s* Bi contribution near E_F. However, for $KBiO_3$ the value of the DOS at E_F, $N(E_F)$, is very sensitive to the method used to generate the DOS. The problem is that, in $KBiO_3$, the SK-DOS positions E_F at the edge of a region where the DOS reduces from 105 to about 1 state/Ry within an energy range of 0.5 mRy. The APW-DOS does not have such a large slope (i.e., flat band) at E_F. This may be due to the rms deviation of 10 mRy between APW and SK, and the small overlap between 3*p* K semicore states and the valence band, which is not included in the SK results.

C. The CPA results

Since the main interest in the Bi-O based cubic perovskites derives from observing superconductivity in $BaPb_{1-x}Bi_xO_3$ (with a maximum $T_c=13$ K for $x=0.3$) and in $Ba_{1-y}K_yBiO_3$ (with a maximum $T_c=30$ K for $y=0.4$), it is important to obtain information on the elec-

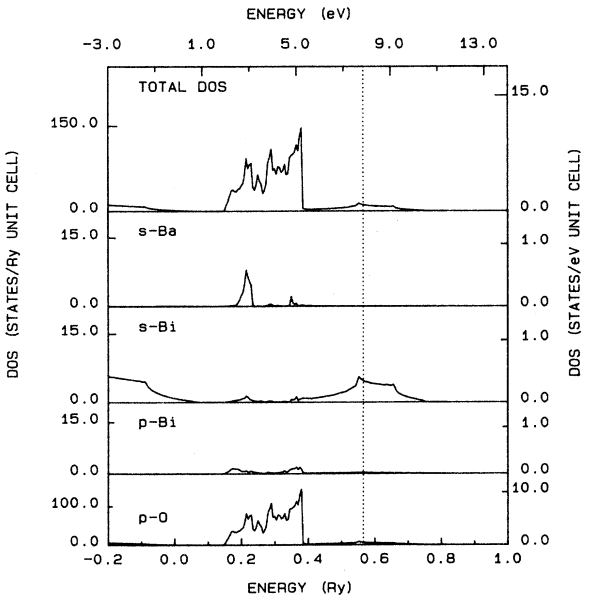

FIG. 7. Slater-Koster densities of state for $BaBiO_3$.

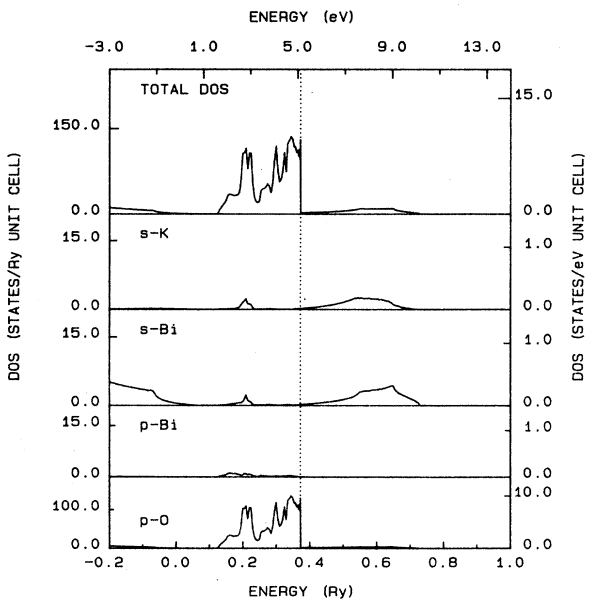

FIG. 8. Slater-Koster densities of state for $KBiO_3$.

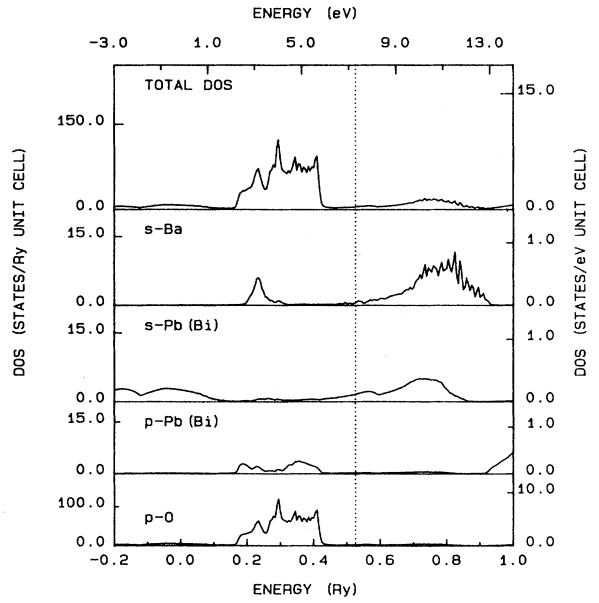

FIG. 9. CPA densities of state for $BaPb_{0.7}Bi_{0.3}O_3$.

tronic structure of these alloys. Mattheiss and Hamann[9,12] addressed this problem using rigid-band arguments and the virtual crystal approximation. This approach often gives an adequate description of the electronic structure of the alloy if the end components of the compositional spectrum have similar band structure. However, the most appropriate method to study the electronic structure of disordered alloys is the CPA.

Our CPA-DOS for $BaPb_{0.70}Bi_{0.30}O_3$ are shown in Fig. 9. A comparison with the DOS of $BaPbO_3$ and $BaBiO_3$ shown in Figs. 6 and 7 confirms some kind of rigid-band description only as far as the position of E_F. The details of the DOS are substantially different between the three calculations and suggest several nonrigid-band features. It is interesting to note that (a) the relative heights of the peaks differ, (b) while the oxygen dominated bandwidth is about the same between $BaPbO_3$ and $BaBiO_3$ it is larger by approximately 0.4 eV for the 30% Bi alloy, (c) the *s* Ba DOS above E_F increases for the alloy in a manner not predictable by a simple interpolation from the end compounds.

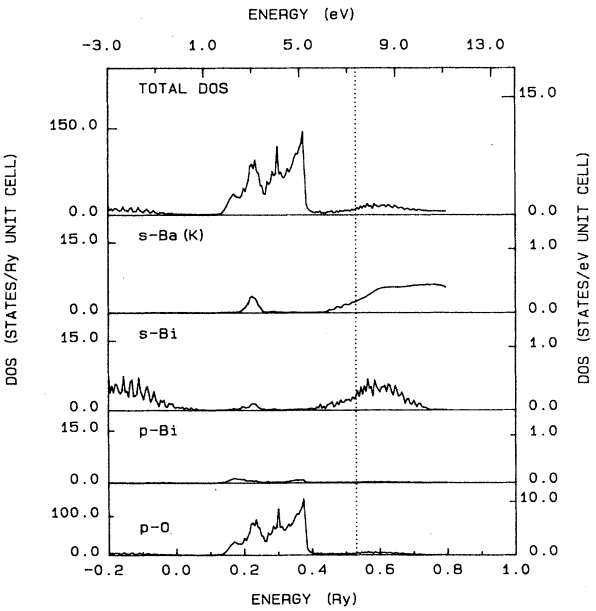

FIG. 10. CPA densities of state for $Ba_{0.6}K_{0.4}BiO_3$.

Our CPA-DOS for $Ba_{0.6}K_{0.4}BiO_3$ are shown in Fig. 10. As in the Pb-based alloy the position of E_F follows rigid-band behavior. However, although the overall structure of the DOS resembles that of $BaBiO_3$, as in the Pb alloys, disorder causes a widening of the bandwidth, by about the same amount. Again *p* O is the dominant component of the DOS, and the *s* Ba(K) contribution is substantial at E_F. This may be crucial in the evaluation of the electron-phonon interaction presented in the next section. The extreme peakiness of some of the component DOS curves for the CPA calculations is numerical noise and should be ignored.

IV. THE ELECTRON-PHONON INTERACTION

These materials seem to become superconductors when the charge-density wave is destroyed. Although the exact superconducting mechanism is still in question some consensus is developing towards the conventional electron-phonon interaction (EPI). According to Mattheiss and Hamann[12] the observed charge-density wave-induced distortion in the semiconducting $BaBiO_3$, suggests that the superconducting properties of the alloys may be explained by the usual (EPI) mechanism. They argue that alloying with K extends the metallic range close to half-filling, where the EPI is strong. Although it is not certain that this picture provides an adequate explanation of superconductivity in these systems, it is very useful to provide a quantitative evaluation of the EPI.

Our approach is to use our band-structure results and calculate the McMillan-Hopfield[18] parameter η in the rigid muffin-tin approximation (RMTA).[19] The reader should be cautioned that there is growing evidence[20] that the RMTA seriously underestimates the value of η. In Table IV we show the values of $\eta=\langle I^2\rangle N(E_F)$ for the stoichiometric compounds that we have studied. It is interesting to see from Table IV that Bi introduces very large increases in both the Bi and O components of η. This increase is mainly caused by a very substantial enhancement of the matrix element $\langle I^2\rangle$ and not of $N(E_F)$. This enhancement of $\langle I^2\rangle$ comes mainly from the *pd* O and the *sp* Bi channels. An observation of the fourth column of Table IV, which gives the η parameters in $KBiO_3$ for an E_F that includes one extra electron (equating the number of valence electrons with those of $BaBiO_3$), indicates a strong EPI in that region. Hence, even without making any correction to the RMTA we find modest values of η which could easily lead to transition temperatures in the observed range if the average phonon frequencies are low in these materials. Indeed,

TABLE IV. Values of $N(E_F)$, Fermi velocity, plasmon energy, and McMillan-Hopfield parameter η in eV/Å^2.

	$BaPbO_3$	$BaBiO_3$	$KBiO_3$	$(KBiO_3)^a$
$N(E_F)$ (states/Ry/unit cell)	10.4	13.6	19.0	11.8
V_f (cm/s)	0.38×10^8	1.57×10^8	0.39×10^8	0.72×10^8
Ω (eV)	1.95	8.82	2.66	3.86
$\eta_{Ba(K)}$	0.0	0.0	0.0	0.0
$\eta_{Pb(Bi)}$	0.055	0.672	0.226	0.721
η_{O_3}	0.472	2.664	0.864	2.723

[a]Corresponding to E_F that contains one extra electron.

we have applied the McMillan equation using the values of η shown in Table IV with $\mu^*=0.1$, and average phonon frequencies 200, 300, and 400 K. The resulting coupling constants λ are 2.4, 1.1, and 0.6, and the superconducting transition temperatures are 26, 19, and 7.5 K, respectively.

V. CONCLUSIONS

We have presented calculations of the band structure of the cubic perovskites $BaPbO_3$, $BaBiO_3$, and $KBiO_3$ by the APW method. Apart from minor differences in detail, our results are in agreement with previous calculations. We have also constructed accurate TB Hamiltonians for these materials by fitting to the APW results. Unlike in previous TB representations, we included s (Ba or K), s and p (Pb or Bi), and p (O) interactions which give a more realistic fit to the APW results. Our CPA results confirmed, at least qualitatively, a rigid-band picture for the position of E_F. However, the CPA yielded a nonrigid-band effect in that the oxygen-dominated valence bands widened by approximately 0.4 eV due to disorder induced by alloying on the Ba and Bi sites. Finally, an evaluation of the parameter η gave values that are large enough to couple with soft phonon modes and result in transition temperatures in the measured range. Thus, the likelihood of conventional electron-phonon mechanism in this system is good.

Recently Shirai *et al.*[21] reported an evaluation of the electron-phonon interaction in the $Ba(K)Pb(Bi)O_3$ system and came to similar conclusions as ours in support of the electron-phonon mechanism. In their paper we found a reference in Itoh *et al.*[22] who reported a Debye temperature of 190 K for $BaPbO_3$. This makes our estimate of an average phonon frequency of 200–300 K realistic, and supports our contention that λ can have a value exceeding 2 in these compounds.

ACKNOWLEDGMENTS

We wish to thank Dr. W. E. Pickett for several discussions and suggestions. This work was partially supported by the U.S. Office of Naval Research and by a National Science Foundation (NSF) supercomputer grant at the University of Illinois.

[1]L. F. Mattheiss, E. M. Gyorgy, and D. W. Johnson, Jr., Phys. Rev. B **37**, 3745 (1988).
[2]R. J. Cava *et al.*, Nature **332**, 814 (1988).
[3]A. W. Sleight, J. L. Gillson, and P. E. Bierstedt, Solid State Commun. **17**, 27 (1975).
[4]S. Pei *et al.*, Phys. Rev. B **39**, 811 (1989).
[5]H. Sato *et al.*, Nature **338**, 241 (1989).
[6]Y. J. Vemura *et al.*, Nature **335**, 151 (1988).
[7]D. G. Hinks *et al.*, Nature **335**, 419 (1988); P. B. Allen, *ibid.* **335**, 396 (1988).
[8]B. Dabronski *et al.*, Physica C **156**, 24 (1988).
[9]L. F. Mattheiss and D. R. Hamann, Phys. Rev. B **28**, 4227 (1983).
[10]D. E. Cox and A. W. Sleight, Solid State Commun. **19**, 969 (1976); Acta. Crystallogr. Sect. B **35**, 1 (1979).
[11]K. Takegahara and T. Kasuya, J. Phys. Soc. Jpn. **56**, 1478 (1987).
[12]L. F. Mattheiss and D. R. Hamann, Phys. Rev. Lett. **60**, 2681 (1988).
[13]J. C. Slater and G. F. Koster, Phys. Rev. **94**, 1498 (1954).
[14]J. S. Faulkner, in *Progress in Materials Science,* edited by J. W. Christian, P. Haasen, and T. B. Massalski (Pergamon, Great Britain, 1982), Vol. 27.
[15]L. Hedin and B. I. Lundqvist, J. Phys. C **4**, 2064 (1971).
[16]L. L. Boyer, Phys. Rev. B **19**, 2824 (1979).
[17]G. Lehmann and M. Taut, Phys. Status Solidi B **54**, 469 (1972).
[18]W. L. McMillan, Phys. Rev. **167**, 331 (1968).
[19]G. D. Gaspari and B. L. Gyorffy, Phys. Rev. Lett. **29**, 801 (1972).
[20]D. A. Papaconstantopoulos, J. Superconductivity **2**, 317 (1989).
[21]M. Shirai, N. Suzuki, and K. Motizuki, J. Phys. Cond. Mater. **1**, 2939 (1989).
[22]T. Itoh, K. Kitazawa, and S. Tanaka, J. Phys. Soc. Jpn. **53**, 2668 (1984).